

Process Simulation Using Abaqus/Explicit Software: Prediction of Cutting Temperatures

Shahmi Shaqir Shaari, Zulaika Zulkifli, Nurul Hayati Abdul Halim*,
Muhammad Raziq Jamaludin, Farrahshaida Mohd Salleh,
Izdihar Tharazi

School of Mechanical Engineering, College of Engineering,
Universiti Teknologi MARA, 40450, Shah Alam, Selangor
*hayatihalim@uitm.edu.my

ABSTRACT

Inconel 718 is a nickel-based superalloy that has good strength even in high temperatures. Therefore it is widely used in aero-engines, heat exchangers and others. Nevertheless, the high-speed machining of Inconel 718 is extremely tricky. Its ability to preserve the mechanical properties at high temperatures and low thermal conductivity, contributes to the inadequate efficiency of the tool. Excessive heat produced during the process of chip forming increases the cutting temperature and accelerates the tool wear. The rapid tool wear resulted in a shorter tool life that significantly increases the cost of the cutting. Thus, this study investigates the influence of different cutting parameters on cutting temperature when high-speed milling Inconel 718 under cryogenic conditions with PVD coated carbide insert. A 3D Finite Element Simulation of the machining process was modelled in Abaqus/Explicit software. Design of Experiment was done through Full Factorial using Design Expert V11 to assimilate 3 factors: cutting speed, V_c (120-140 m/min), feed rate, f_z (0.15-0.25 mm/tooth), and axial depth of cut, a_p (0.3-0.7 mm) which required a total of 8 sets of process parameters while the radial depth of cut, a_e is fixed at 0.4 mm. Analysis of Variance (ANOVA) shows that a_p and f_z are the significant factors that influence the cutting temperature. a_p is the most significant parameter with a contribution of 81.11%. The increase of a_p results in an increase in cutting temperature. The optimization required for minimum cutting temperature was suggested at V_c : 140 m/min, f_z : 0.15 mm/tooth, and a_p : 0.3 mm to achieve temperature as low as 413.3 °C. By using these optimum parameters, the low cutting temperature can be achieved which will result in longer tool life while maintaining high-speed milling for a high production rate, especially in aerospace industries.

Keywords: *High-speed milling; Inconel 718; Cryogenic cutting; 3D FE simulation; Cutting temperature*

Introduction

Inconel 718 is a nickel-based heat resistance superalloy (HRSA) that is also recognized as a difficult-to-cut material. This material has a very good strength even in high temperatures. Its melting range is around 1330 °C to 1375 °C [1]; therefore, it is widely used in the aviation industry such as aero-engines, gas turbine engines, combustion cans and ducts, and high-temperature applications like heat exchangers, heat-treating equipment, petrochemical processing, power plant equipment and catalyst-grid support in nitric acid production. The primary characteristic of Inconel 718 which is high strength in extremely high temperature and high resistance of corrosion makes it one of the best materials to be used for extreme service environments. While the drawback of its primary features is the difficulty of the machine in high-speed conditions because it has high work-hardening and low thermal conductivity [2]. Cutting tools are often get worn out immediately when machining Inconel 718 [3]. When the cutting tools get worn out, it will lead to high surface roughness which will reduce the quality of the finishing [4].

One of the important factors in the machining process is the cutting parameters. If the most suitable cutting parameters are selected, it will produce a high-quality surface finish with consideration in shape, size, and tolerance. Toubhans et al. [5] conducted a study focused on the cutting force contemplating tool wear and the influence on surface quality. The study analysed the impact of cutting parameters and tool wear on residual stress profiles in the machining affected area. The study found that tool wear has a significant effect on cutting forces and surface quality. The residual stresses profiles that have been achieved with worn tools display a highly compressive state in the subsurface combined with elevated tensile stress close to the machined surface. By applying a high level of cutting speeds and low feed rate, the compressive stress at the surface and the affected depth in the controlled wear region can be reduced

Cutting condition or in other words, cooling mechanism, plays a big role in extending the cutting tool life [6]. Cutting condition in milling processes is influenced by the workpiece material, operation types, and cutting tool selection. In industries, the most used are cutting fluid and dry cutting conditions. Cutting fluid, whether coolant or lubricant, is dependent on the machining operation since excessive usage of the fluid can affect tool wear and workpiece surface finish. It also prevents an undesirable chip from interfering with the cutting operation by dragging it away. Several cooling mechanisms were used in past studies such as cryogenic condition, minimum quantity lubrication (MQL), dry cutting, flood cutting, conventional and

hybrid cutting conditions. Past studies show that flood cutting conditions are the best cooling mechanism compared to others [7]. Unfortunately, there are disadvantages of flood cutting conditions as it is very costly to recycle and to dispose of. Not only that, but it is also not very environmentally friendly, as nowadays, the industries prefer more eco-friendly manufacturing processes [6]. Because of that, dry machining was introduced in industries. Cryogenic cutting condition is the most efficient and more eco-friendly compared to others [8]. A study by Halim et al. [9] finds that that cryogenic condition produces an efficient cooling effect at the cutting zone. There are two types of cryogenic cutting conditions which is CO₂ and LN₂. Cryogenic CO₂ leads to a slower rate of tool wear in comparison to the cryogenic LN₂ [10]. Therefore, cryogenic CO₂ cutting condition is the best option. Cryogenic CO₂ demonstrated significant improvement towards maximizing the tool life to 70.8% compared to dry cutting. Constant cryogenic CO₂ cooling efficiently lowers the cutting temperature to effectively 80% relative to dry cutting.

Few control factors influence the cutting tool life and temperature which are cutting speed, feed rate, and depth of cut. The axial depth of cut is the primary factor controlling the cutting forces followed by the interactivity between feed rate and radial depth of cut [9]. With the axial depth of cut, the forces were greatly improved due to the rise in the size of the cut by the insert. Hafiz et al. [11] stated that all control factors which are cutting speed, feed rate, and cutting conditions significantly affect the tool life, surface roughness and cutting force applied during the face milling process. The feed rate was founded to be the most significant factor. When the feed rate increase, the heat produced in the cutting area also increase and caused the deformation of cutting tool edge which resulted in rapid tool wear. High cutting speed of Inconel 718 has been proven to produce not quite good result for surface roughness due to high rate of tool wear for the following cut. In the other hand, low cutting speed shows no main sign of tool damages are detected, and the tool life are longer [3]. Higher feed rate and higher depth of cut also contribute to less tool life [12].

Tool wear also influenced by the coating of the cutting insert. Prabha et al. [13] conducted a comparative study to investigate the wear patterns of both coated and uncoated tool inserts in the high-speed turning of EN36 steel. The study shows that coated tool inserts performed highly better compared to uncoated at higher speeds. A study by Sampath et al. [14] finds that TiAlN/AlCrN bi-layer coated tool shows a better performance during machining process when compared to TiAlN, AlCrN coated and uncoated carbide tool for machining Inconel 825 alloy. These studies proved that coated cutting tools perform better than uncoated ones. Hardness, tool life, quality on machining surfaces and wear resistance are all improved by coatings.

During the machining process, the friction between the workpiece and the tool created a heat load in the cutting zone. The chip generation, wear

mechanism, and surface roughness of machined parts are all influenced by the rise in temperature in the cutting zone. As shown in Figure 1, there are three zones which are primary deformation zone (Zone 1), secondary deformation zone (Zone 2), and tertiary deformation zone (Zone 3) where heat was generated during the machining process [15]. A research that was performed by Fahad [15] finds that the most critical zone where heat is generated is at the secondary deformation zone (Zone 2) caused by the friction between the tool face and the chip while the wear of the tools occurs at the tertiary deformation zone (Zone 3) caused by the interaction between workpiece surface with the flank face of cutting tool.

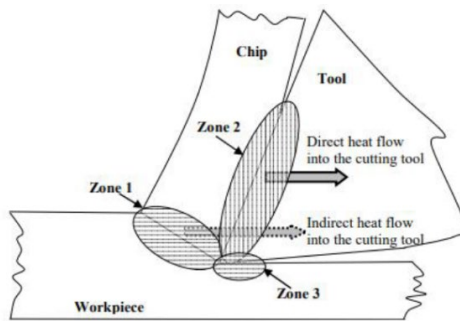


Figure 1: Heat generation in cutting zone [15]

Typically, when the temperature increase, the yield strength of the majority of all engineering material decreased as shown in Figure 2. The removal of work material is easier when the cutting temperature is higher. To achieve an energy-efficient of machining process, it is necessary to manage the cutting temperature to soften the work material while maintaining the mechanical strength of tool materials [16]. The workpiece burn and stress concentration will lower the workpiece's service time, increasing maintenance costs and reducing machining efficiency [17]. Based on previous studies, the cutting temperature can be controlled by controlling the cutting parameters. According to Wang et al. [16], the most significant factor that influenced cutting temperature is the cutting speed. By controlling the cutting speed, the highest energy efficiency of machining can be achieved. While a study conducted by Liu et al. [17] shows that cutting speed and depth of cut are the parameters that affected cutting temperatures. According to the study, when the cutting speed is at a low level, the cutting speed is the significant factor that affects the cutting temperature while when the level of depth of cut is high, the depth of cut is the major factor affecting the cutting temperature.

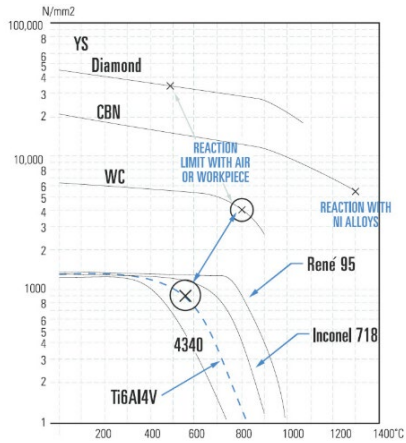


Figure 2: Yield strength of work material and tool at different temperatures [16]

As technology advances in the engineering sector, the software is being developed as a tool for practising analysis and simulation, prediction, and optimization for all problems. Simulation is used in the machining industry to examine machining performance, operations, and to optimise output for economic reasons. It also makes it easier for experts and engineers to avoid the time-consuming trial-and-error procedure, which reduces the manufacturer's output. Davim et al. [18] conducted research on precision radial turning of AISI D2 steel, intending to compare finite element model (FEM) simulations to experimental and analytical findings. Regardless of the friction coefficient employed in the simulation study, the results demonstrate that the difference between the experimental and modelled cutting force is about 20%. A three-dimensional (3D) finite element (FE) simulation model was developed by Zhang et al. [19] to study the cutting forces and cutting temperature in hard milling of AISI HI3 steel. By the comparison between the simulated cutting forces to the experiment data, the simulation model's prediction validation for the hard milling process was confirmed.

The main objectives of this project are to investigate the effects of cutting parameters on cutting temperatures when using Abaqus/Explicit software to simulate high-speed milling of Inconel 718 and to analyse the influence of milling parameters on cutting temperatures. The optimum milling parameters are then identified by using ANOVA.

Methodology

Model of Milling Inserts for FEA

Milling inserts are bits that are replaceable and used to machine some of the hardest materials. In the actual process, the milling cutter holder in which the inserts are attached rotates around the axis of the cutting tool. An H-hexagon Wave Mill WEZ Indexable Tungsten Carbide insert as shown in Figure 3(a) was used for the high-speed milling process simulation in this study. Figure 3(b) shows the insert geometry as created in Abaqus pre-processing modelling.

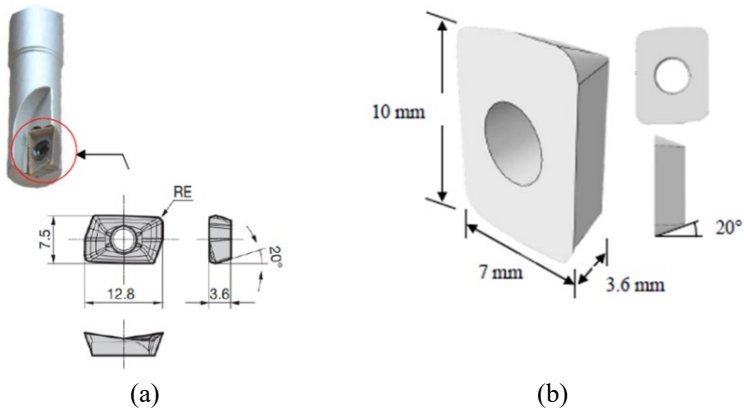


Figure 3: Cutting tool model (a) Actual machining cutting tool (b) Tool insert geometry

Indexable Endmills in Sumitomo Catalogue was referred to for the geometry and material of the insert. According to the manufacturers, this insert is useable in a wide range of machining processes and various materials [20]. Table 1 shows the properties of PVD coated carbide insert [20], [21].

Table 1: Properties of PVD coated carbide [20], [21]

Elastic Modulus, E (GPa)	800
Poisson's Ratio, σ	0.2
Thermal Expansion (mm/mm*°C)	4.7e-06
Thermal Conductivity (W/m °C)	47
Density (kg/m ³)	15000
Specific heat (J/kg)	203

Model of Workpiece for FEA

Figure 4 shows the model of the workpiece that was created in the Abaqus software. The chemical composition of the chosen material which is Inconel 718 is shown in Table 2. Two sections were created on the workpiece which is the upper and lower section. A revolve cut section was created on the upper section to obtain as close as possible to the actual milling process. During the simulation, the insert simulated rotational cutting process along the upper section. The properties of Inconel 718 are shown in Table 3 [22].

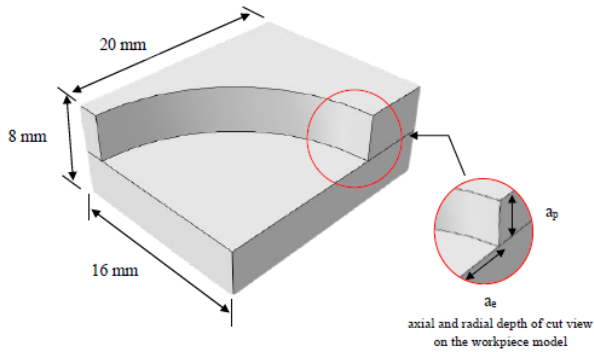


Figure 4: Workpiece geometry

Table 2: Composition of Inconel 718 [8]

Ni	Cr	Fe	Nb	Cu	Al	B	C	Co
53	18.30	18.70	5.05	0.04	0.49	0.004	0.051	0.3
Mo	Ti	Mn	Si	S	P			
3.05	1.05	0.23	0.08	<0.002	<0.005			

Table 3: Properties of Inconel 718 [22]

Thermal Conductivity, γ (W/m ² °C)	11.4
Density, (kg/m ³)	8195
Thermal Expansion Coefficient, (10 ⁻⁶ /°C)	11.5
Specific Heat, (J/kg/°C)	430
Young Modulus, E (MPa)	200 000
Poisson's Ration, σ	0.3
Melting Point, (°C)	1260

Material Constitutive Model of the Workpiece

For this study, the Johnson-Cook model was applied in the simulation. According to Zhang et al. [19], the Johnson-Cook model is a method that is effective to be used in finite element analysis of the machining process. Johnson-Cook model can be explained as shown in Equation (1). A, B, C, m, and n are material constant, σ is equivalent stress, ϵ is the equivalent strain, $(\dot{\epsilon})$ is plastic strain rate, is reference strain rate $\dot{\epsilon}_0$, T_0 is reference temperature, and T_{melt} is melting temperature. Table 4 and Table 5 show the plasticity and failure parameters that were referred for the simulation.

$$\sigma = (A + B_{\epsilon^n}) \left[1 + C \left(\frac{\ln \dot{\epsilon}}{\dot{\epsilon}_0} \right) \right] \left[1 - \left(\frac{T - T_0}{T_{melt} - T_0} \right)^m \right] \quad (1)$$

Table 4: Johnson-Cook plasticity parameters [22]

A (Mpa)	B (Mpa)	n	m	Melting Temp. (°C)	Transition Temp. (°C)
980	1370	0.164	1.03	1260	25

Table 5: Johnson-Cook failure parameters [22]

d1	d2	d3	d4	d5	Melting Temp. (°C)	Transition Temp. (°C)
0.11	0.75	-1.45	0.04	0.89	1260	25

Geometric Modelling and Meshing

In the meshing section, a visual of the workpiece and cutting tool was created. A total of 6829 workpiece nodes and 5515 elements were generated using linear hexahedral elements of type C3D8RT for a more efficient and precise modelling process. It meshes section generated a total of 552 nodes and 335 elements for the cutting tool insert, as illustrated in Figure 5.

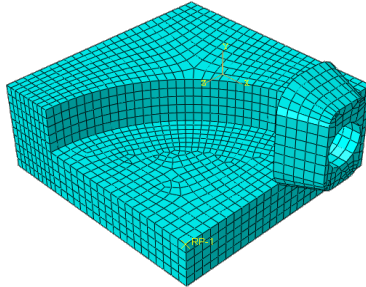


Figure 5: Meshing section of machining simulation

Boundary conditions for both the cutting tool and the workpiece are shown in Figure 6. A boundary condition of symmetry/ antisymmetry/ encaster is chosen, which constrains all active structural degrees of freedom in the defined region. As a result, the displacement perpendicular to the plane and the rotational vector components parallel to the plane are both zero. To generate cutting tool rotational movement along with the work material, the angular velocity/velocity is chosen as the boundary condition. The tool's cutting speed was set in the boundary section.

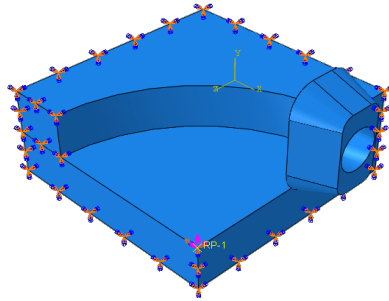


Figure 6: Boundary condition

On the corner edge of the workpiece cut section, a reference point 1 was chosen, as shown in Figure 7. In the constraint section, a pair of kinematical points were generated, then a linear feed and a rotation were applied at the reference point to construct a rotation motion. The cutting tool revolves around the y-axis of the reference coordinate system during the simulation, causing the cutting speed and feed rate to be simulated through tool motion. As the tool insert cuts along the workpiece, a motion along the z-axis is called a feed rate. In this modelling simulation, the start temperature for both the workpiece and the cutting insert in the designated field area was set to 25 °C. A CO₂ cryogenic cooling was also simulated by applying a surface film condition at the surface of the cutting tool. The CO₂ cryogenic temperature was set at -78.5 °C [23].

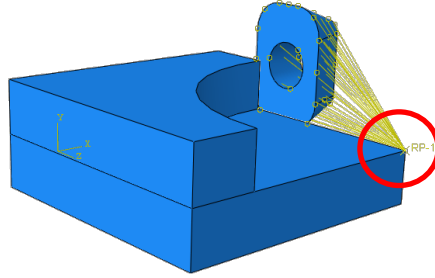


Figure 7: Finite element model configuration

Experiment Setup

The independent variable in analysing heat generated during machining simulation is the machining parameter, which includes cutting speed, feed rate, axial, and radial depth of cut. Table 6 shows the range of parameters chosen based on Halim et al. [8] for computational simulation and experiment results as references. For both levels of the experiment, the radial depth of cut was kept constant at 0.4 mm.

Table 6: Cutting parameters used

Variable Parameters	Level of Experiment	
	Low	High
Cutting speed, V_c (m/min)	120	140
Feed rate, f_z (mm/tooth)	0.15	0.25
Axial depth of cut, ap (mm)	0.3	0.7
Radial depth of cut, ae (mm)	0.4 (fixed)	

The design of the experiment was conducted using the Full Factorial method in Design Expert V11 software. The Design Expert V11 software can conduct a thorough experiment on the process and a variety of factors and components. Design Expert also simplifies data analysis by correctly generating statistical models in the form of charts, graphs, and tables. To identify the interaction between the factors and the level of the experiment, ANOVA was applied. Table 7 shows a total of 8 experiments were conducted with different machining variables for the optimization process. Optimum milling parameters to achieve the lowest cutting temperatures while maintaining the high speed of the milling process were identified by using Analysis of Variance (ANOVA). The ANOVA is carried out for a level of significance of 5%, i.e., for a level of confidence of 95%.

Table 7: Full Factorial design

No. of run	Factor A: Cutting speed (m/min)	Factor B: Feed rate (mm/tooth)	Factor C: Axial DOC (mm)	Factor D: Radial DOC (mm)
1	140	0.25	0.7	
2	140	0.15	0.7	
3	120	0.15	0.3	
4	120	0.25	0.7	0.4
5	120	0.15	0.7	
6	140	0.25	0.3	
7	140	0.15	0.3	
8	120	0.25	0.3	

Results and Discussion

Table 8 displays the result of cutting temperature obtained from 8 experiments with different cutting speeds, feed rate and axial depth of cut, and at a fixed radial depth of cut under cryogenic CO₂ cooling. The cutting temperature was measured in degree Celsius (°C) on FE simulation.

Table 8: Temperature result in different parameters on FE simulation

No. of run	Factor A: Cutting speed (m/min)	Factor B: Feed rate (mm/tooth)	Factor C: Axial DOC (mm)	Factor D: Radial DOC (mm)	Response: Cutting temperature (°C)
1	140	0.25	0.7		624.2
2	140	0.15	0.7		507.2
3	120	0.15	0.3		418.6
4	120	0.25	0.7	0.4	619.2
5	120	0.15	0.7		535.6
6	140	0.25	0.3		460.9
7	140	0.15	0.3		408
8	120	0.25	0.3		401.6

Influence of Cryogenic CO₂ Cooling

A dry cutting simulation was also generated by using Abaqus/Explicit software to compare the cutting temperature difference between dry cutting and cryogenic. However, the results of the cutting temperature under dry cutting are not shown as it is not in the scope of this project. The comparison of cutting temperature under both cutting conditions shows that the cryogenic CO₂ coolant influenced the cutting temperature by reducing it 5% - 10% of the cutting temperature under dry cutting. The lack of coolants in dry cutting exposes the tool to higher temperatures due to the considerable heat and friction generated during the cutting process.

These findings are almost similar to the one reported by Dilip and Paradeep [24], which stated that the implementation of CO₂ reduced the cutting temperature by about 6% - 21%. On the other hand, there is a huge difference with the results obtained from the experimental works conducted by Halim et al. [25] and Cordes et al. [26]. Halim et al. [25] stated that the cryogenic CO₂ succeed to reduce the cutting temperature significantly by 80% while Cordes et al. [26] finds that the cutting temperature was reduced by 43% - 55% under the same cutting condition. Nevertheless, all these findings agree that cryogenic CO₂ cooling can be reduced cutting temperatures which will slow the tool ware rate and increase the tool life and surface quality. It is also important to note that the huge difference in the measured cutting temperatures between the simulation and experimental results might be happened due to the fog of the CO₂ flow that covered the cutting area during cutting, thus reduced the measurement accuracy of the infrared thermal image camera. Therefore, Musfirah [27] recommends the use of thermocouple sensor which contact with the cutting tool, for more accurate measuring process during the experimental works.

Analysis of Variance (ANOVA)

Table 9 shows the result of ANOVA. From the analysis, the Model F-value of 32.85 implies the model is significant. P-values less than 0.05 indicate model terms are significant. Based on the table, parameters which are feed rate (B), axial depth of cut (C) and the interaction between both parameters (BC) are significant model terms.

Table 9: Analysis of Variance (ANOVA)

Source	Sum of Squares	df	Mean Square	F-value	p-value	Contribution %
Model	54948.34	3	18316.11	32.85	0.0028	significant
B	6991.53	1	6991.53	12.54	0.0240	12.72
C	44566.05	1	44566	79.93	0.0009	81.11
BC	3390.76	1	3390.76	6.08	0.0692	6.17
Residual	2230.21	4	557.55			
Cor Total	57178.55	7				

The most dominant parameter that influences cutting temperature is the axial depth of cut with the highest contribution of 81.11% where the P-value is 0.0009, less than 0.05 which indicate that it is a significant term. Similar to the findings by Halim et al. [9] which the axial depth of cut was found to be the most dominant factor determining cutting forces. The forces increased substantially with the axial depth of cut caused by the increase of the size of cut by the insert. The high forces caused extreme temperatures during the machining process. A study by Pereira et al. [23] agreed that the

cutting temperatures increase along with the increase of cutting force which will also increase the tool wear rate.

Feed rate was the second significant factor influencing the cutting temperature with a contribution of 12.72%. Cutting speed is not included in the table because the P-value is greater than 0.05 which makes it not a significant factor towards the response. The percentage of factors contributing to cutting temperature was calculated from the sum squares for the term relative to the total sum of squares. Figure 8 shows the graph of interaction between each significant factor, axial depth of cut and feed rate, with the cutting temperature. The slope of the graphs shows that axial depth of cut, Figure 8(a), is a factor that is more significant compared to feed rate, as in Figure 8(b).

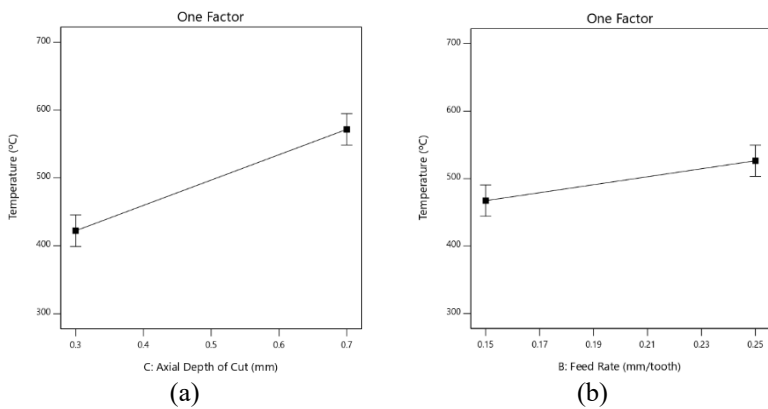


Figure 8: One factor (a) Axial depth of cut (b) Feed rate

The interaction between axial depth of cut and feed rate also considered a significant factor because the p-value is only slightly more than 0.05. Figure 9 shows the 3D surface plot of the interaction between the cutting parameters and the response measured. For the initial run of the simulation, the axial depth of cut and feed rate was set to 0.3 mm and 0.15 mm/tooth respectively. In general, by decreasing both factors, the cutting temperature can be reduced to the lowest. Based on the red temperature contour, when the axial depth of cut and feed rate increase, the cutting temperature also increases.

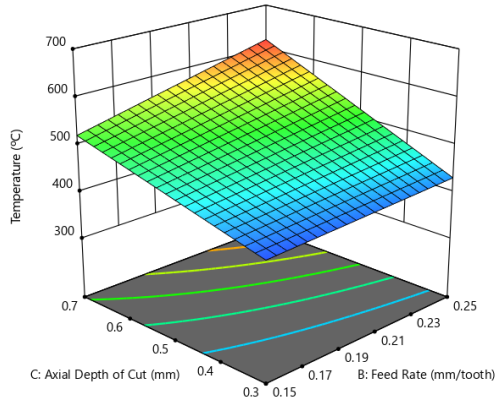


Figure 9: 3D surface plot of the interaction of axial DOC and feed rate

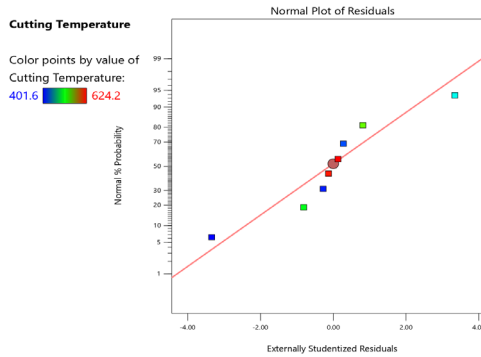
A second-order statistical equation model was developed by multiple regression and expressed in actual factors as shown in Equation 2. For the given values of each factor, the equation in terms of actual factors can be used to generate predictions about the response. For each factor, the levels should be indicated in the original units. Because the coefficients are scaled to suit the units of each element and the intercept is not at the centre of the design space, this equation should not be used to evaluate the relative impact of each factor.

Cutting Temperature

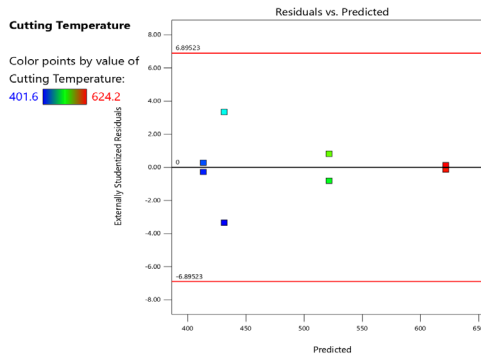
$$= 397.94375 - 438.125fz - 38.5625ap + 2058.75fz * ap \quad (2)$$

Verification of the Model

The diagnostic plot of the normal plot of residuals and residual vs predicted plot was analyzed as shown in Figure 10 to verify the data was fit and acceptable. Based on the normal plot of residuals in Figure 10(a) shows that all the residual data were close to the line which indicates that data are consistent with normal distribution as stated by Halim et al. [9]. The residual vs predicted plot in Figure 10(b) shows that there are no obvious pattern and unusual structure model as all the data are within the limits.



(a)



(b)

Figure 10: Model diagnostic (a) Normal plot of the model and (b) Residual vs Predicted

Optimization of Cutting Temperature

A total of 89 solutions were generated to get the optimum value of parameters to produce the lowest cutting temperature. The cutting speed was set to the middle of the range since the factor is not significant. Table 10 shows 7 of the solutions generated. Solution number 1 with optimum milling parameters V_c : 140 m/min, f_z : 0.15 mm/tooth and ap : 0.3 mm was chosen as it can produce the lowest cutting temperature which is 413.3 °C and have the highest desirability of 0.947.

Table 10: Optimization solution for cutting temperature

No.	Cutting Speed (m/min)	Feed Rate (mm/tooth)	Axial DOC (mm)	Radial DOC (mm)	Temperature (°C)	Desirability	
1	140.000	0.150	0.300	0.4	413.300	0.947	Selected
2	120.000	0.150	0.300	0.4	413.300	0.947	
3	133.427	0.150	0.300	0.4	413.300	0.947	
4	130.696	0.150	0.300	0.4	413.300	0.947	
5	129.110	0.150	0.300	0.4	413.300	0.947	
6	135.820	0.150	0.300	0.4	414.300	0.947	
7	121.984	0.150	0.300	0.4	414.300	0.947	

Temperature Distribution of the Model

As can be seen in Figure 11, the time start for the temperature to rise from initial is different as stated by Qing Zhang et al. [19] in their study of 3D FE simulation of high-speed and hard milling. This happens because the initial position of the tool insert is not the same as the axial depth of cut of every simulation is different and the temperature rises along the cutting zone.

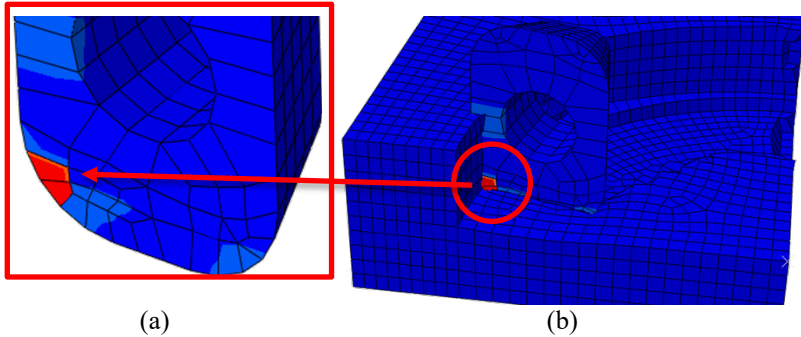


Figure 11: Temperature distribution at (a) Cutting tool edge and (b) Tool-chip surface (V_c : 140 m/min, f_z : 0.25 mm/tooth, a_p : 0.7 mm)

Figure 11(b) indicates that the highest cutting temperature of 624.2 °C was recorded at the contact zone between the workpiece and the cutting tool according to the red temperature contour. The maximum temperature was generated at the secondary deformation zone which is the most critical zone as described by Fahad [15]. The thermal load created by the friction between the cutting tool face and the workpiece causes the temperature to rise. Heat is produced at the secondary deformation zone as a result of the work done to overcome the sliding friction of tool-chip contact, which causes crater wear. Inconel 718 with poor thermal conductivity and high-temperature strength resulted in low heat output from the cutting zone. The heat that

accrued at the cutting zone raised the cutting temperature, causing work hardening of the material as stated by Halim et al. [8].

As shown in Figure 11(a) the simulation illustrates that the temperature distribution is near to the cutting edge of the tool insert. The increase of axial depth cut increases the contact length which leads to the rise of cutting temperature. A study by Toh [28] agrees that the axial depth of cut influence the cutting temperature significantly caused by the increase of contact area. The high temperature in the cutting zone causes the tool to lose its strength, which leads to plastic deformation.

The increase of temperature in the cutting zone resulted in a high tool wear rate and surface roughness of machined parts. This condition has been reported by [15], [8], [29]. Unfortunately, the chip formation was unable to be generated in this FE simulation due to the limitation of the simulation (the chip formation element in this zone is deleted throughout the FE simulation process).

Conclusion

This project main focus is to study the effects of cutting parameters towards cutting temperature of high-speed milling of Inconel 718 by using PVD coated carbide insert. FE simulation and design of experiment (DOE) were applied in this study to investigate the correlation between cutting parameters with cutting temperatures under cryogenic CO₂ cooling in a milling nickel-based superalloy. A full factorial method was used which developed a total of 8 experiments with different cutting parameters that need to be conducted. The results obtained from the simulation was analyzed and verified by the Analysis of Variance (ANOVA) to identify the relation between cutting parameters and cutting temperature to obtain process optimization.

From the results obtained, it was discovered that the cryogenic CO₂ influenced the cutting temperature by reducing it by 5% - 10% compared to dry cutting. The axial depth of cut shows the most significant factors that influence the cutting temperature followed by the feed rate with the contribution of 81.1% and 1.27% respectively. However, cutting speed seems to have no significant impact on cutting temperature. The optimum parameters were generated by ANOVA to achieve the lowest cutting temperature while maintaining a high cutting speed for the milling process. The most optimum parameters with 0.947 desirability are V_c : 130 m/min, f_z : 0.15 mm/tooth and a_p : 0.3 mm. The presented 3D FE simulation can assist to better understand the system of the high-speed milling process and aids to optimize cutting parameters such as feed rate, depth of cut and radial depth of cut.

References

- [1] G. Li, Z. Liu, B. Wang, Y. Liu, and J. Zhao, "Effect of element Te on alterations of microstructure and mechanical property of nickel-based superalloy Inconel 718 through alloy infiltration," *Appl. Surf. Sci.*, vol. 544, p. 148730, 2021.
- [2] C. Liu, M. Wan, W. Zhang, and Y. Yang, "Chip Formation Mechanism of Inconel 718: A Review of Models and Approaches," *Chinese J. Mech. Eng. (English Ed.)*, vol. 34, no. 1, 2021.
- [3] D. M. D'Addona, S. J. Raykar, and M. M. Narke, "High Speed Machining of Inconel 718: Tool Wear and Surface Roughness Analysis," *Procedia CIRP*, vol. 62, pp. 269–274, 2017.
- [4] N. Potthoff and P. Wiederkehr, "Fundamental investigations on wear evolution of machining Inconel 718," *Procedia CIRP*, vol. 99, pp. 171–176, 2021.
- [5] B. Toubhans, G. Fromentin, F. Viprey, H. Karaouni, and T. Dorlin, "Machinability of inconel 718 during turning: Cutting force model considering tool wear, influence on surface integrity," *J. Mater. Process. Technol.*, vol. 285, 2020.
- [6] K. Venkatesan, "The study on force, surface integrity, tool life and chip on laser assisted machining of inconel 718 using Nd:YAG laser source," *J. Adv. Res.*, vol. 8, no. 4, pp. 407–423, 2017.
- [7] M. A. Xavier, M. Manohar, P. Jeyapandiarajan, and P. M. Madhukar, "Tool Wear Assessment during Machining of Inconel 718," *Procedia Eng.*, vol. 174, pp. 1000–1008, 2017.
- [8] N. H. B. Abdul Halim, C. H. Che Haron, J. A. Ghani, and M. F. Azhar, "Tool life prediction by RSM for cryogenic milling of inconel 718," *Ind. Lubr. Tribol.*, vol. 73, no. 1, pp. 8–14, 2021.
- [9] N. Hayati, A. Halim, C. Hassan, C. Haron, J. A. Ghani, and M. F. Azhar, "Prediction of Cutting Force for Milling of Inconel 718 under Cryogenic Condition by Response Surface Methodology," vol. 16, no. 1, pp. 1–16, 2019.
- [10] N. H. A. Halim, C. H. C. Haron, J. A. Ghani, and M. F. Azhar, "Tool wear and chip morphology in high-speed milling of hardened Inconel 718 under dry and cryogenic CO₂ conditions," *Wear*, vol. 426–427, pp. 1683–1690, 2019.
- [11] M. S. A. Hafiz, W. N. F. Mohamad, Nu. S. M. Zainurin, M. Akmal, R. Izamshah, and S. B. Mohamed, "Machinability of Inconel 718 during face mill," *Proc. Asia Int. Conf. Tribol. 2018*, no. September, pp. 369–370, 2018.
- [12] A. A. Chavan and P. V. Deshmukh, "Prediction of tool life of different coated cutting tools during machining of Inconel 718," *Int. Res. J. Eng. Technol.*, vol. 4, no. 12, pp. 941–949, 2017.
- [13] K. Aruna Prabha, B. Srinivasa Prasad, and N. Srilatha, "Comparative

- Study of Wear Patterns of both Coated and Uncoated Tool Inserts in High Speed Turning of EN36 Steel,” *Mater. Today Proc.*, vol. 5, no. 2, pp. 4368–4375, 2018.
- [14] S. K. T. *et al.*, “Comparative evaluation of performances of TiAlN, AlCrN, TiAlN/AlCrN coated carbide cutting tools and uncoated carbide cutting tools on turning Inconel 825 alloy using Grey Relational Analysis,” *Sensors Actuators, A Phys.*, vol. 279, pp. 331–342, 2018.
- [15] M. Fahad, “A Heat Partition investigation of Multilayer Coated Carbide Tools for High Speed Machining through experimental studies and Finite Element Modelling A thesis submitted to for the degree of In the Faculty of Engineering and Physical Sciences Muhammad Fahad,” no. January 2012, 2012.
- [16] Z. Wang, S. Nakashima, and M. Larson, “Energy efficient machining of titanium alloys by controlling cutting temperature and vibration,” *Procedia CIRP*, vol. 17, pp. 523–528, 2014.
- [17] C. Liu *et al.*, “Effects of process parameters on cutting temperature in dry machining of ball screw,” *ISA Trans.*, vol. 101, pp. 493–502, 2020.
- [18] J. P. Davim, C. Maranhão, P. Faria, A. Abrão, J. C. Rubio, and L. R. Silva, “Precision radial turning of AISI D2 steel,” *Int. J. Adv. Manuf. Technol.*, vol. 42, no. 9–10, pp. 842–849, 2009.
- [19] Q. Zhang, S. Zhang, and J. Li, “Three Dimensional Finite Element Simulation of Cutting Forces and Cutting Temperature in Hard Milling of AISI H13 Steel,” *Procedia Manuf.*, vol. 10, pp. 37–47, 2017.
- [20] M. Tools, “G-j 20|21.”
- [21] K. Nasralla, S. K. Shihab, and A. K. Mahmoud, “Finite Element Modeling and Optimization of Estimated Cutting Forces during Machining of Inconel 718,” *Int. J. Mater. Sci. Eng.*, vol. 4, no. 3, pp. 1–7, 2018.
- [22] A. K. Kumar and P. Venkataramaiah, “Heat assisted machining of inconel 718 Alloy using abaqus/explicit,” *Mater. Today Proc.*, vol. 18, pp. 4531–4536, 2019.
- [23] O. Pereira, A. Celaya, G. Urbikaín, A. Rodríguez, A. Fernández-Valdivielso, and L. Noberto López de Lacalle, “CO2 cryogenic milling of Inconel 718: Cutting forces and tool wear,” *J. Mater. Res. Technol.*, vol. 9, no. 4, pp. 8459–8468, 2020.
- [24] B. Dilip Jerold and M. Pradeep Kumar, “Experimental comparison of carbon-dioxide and liquid nitrogen cryogenic coolants in turning of AISI 1045 steel,” *Cryogenics (Guildf.)*, vol. 52, no. 10, pp. 569–574, 2012.
- [25] N. H. A. Halim, C. H. C. Haron, J. A. Ghani, and M. F. Azhar, “Tool wear and chip morphology in high-speed milling of hardened Inconel 718 under dry and cryogenic CO2 conditions,” *Wear*, vol. 426–427, pp. 1683–1690, Apr. 2019.
- [26] S. Cordes, F. Hübner, and T. Schaarschmidt, “Next generation high performance cutting by use of carbon dioxide as cryogenics,” *Procedia*

- CIRP*, vol. 14, pp. 401–405, 2014.
- [27] M. B. A. Hadi, “Pencirian dan analisa pemesinan laju tinggi kriogenik menggunakan mata alat kisar hujung bebola bersalut karbida ke atas Inkonel 718,” Universiti Kebangsaan Malaysia, 2016.
- [28] C. K. Toh, “Comparison of chip surface temperature between up and down milling orientations in high speed rough milling of hardened steel,” *J. Mater. Process. Technol.*, vol. 167, no. 1, pp. 110–118, 2005.
- [29] N. A. Abukhshim, P. T. Mativenga, and M. A. Sheikh, “Heat generation and temperature prediction in metal cutting: A review and implications for high speed machining,” *Int. J. Mach. Tools Manuf.*, vol. 46, no. 7, pp. 782–800, 2006.